Role of complexing agents in the appearance of Turing patterns

Damián E. Strier* and Silvina Ponce Dawson†
Departamento de Física, Facultad de Ciencias Exactas y Naturales, UBA, Ciudad Universitaria, Pabellón I, (1428) Buenos Aires, Argentina
(Received 19 November 2003; published 4 June 2004)

In this paper we study a four-species reaction-diffusion system where Turing patterns are stabilized by the presence of fast reversible reactions between the morphogens and two different mobile complexing agents (CAs) that are not necessarily in excess. We provide a quantitative explanation of how the interaction with the CA changes the size of the Turing space making it possible to observe patterns even in a region where the free diffusion coefficients of the relevant species are equal, as is usually the case in real systems. Our analytical treatment gives a series of mathematical relations that can be helpful for those designing experiments where Turing patterns are expected to appear. We also show how the mobility of CAs affect the characteristic size of the pattern. Finally, we provide an example of biological interest in order to illustrate the main procedures and results.

DOI: 10.1103/PhysRevE.69.066207 PACS number(s): 05.45.−a, 82.40.Ck, 89.75.−k, 82.39.−k

I. INTRODUCTION

Self-organization far from thermodynamic equilibrium [1] is an active area of research in an increasing number of fields, such as fluids, optics, biophysics, and physical chemistry. Among the diversity of pattern formation phenomena, the spontaneous diffusive instabilities of an homogeneous mixture in reaction-diffusion systems, first proposed theoretically by Turing [2], remains as a paradigmatic example (see Ref. [3] for a recent review). The Turing instability, spontaneously leads to chemical concentration structures, which are space periodic, time stationary, and possess an intrinsic wavelength. The symmetry breaking of an homogeneous state has to involve three unavoidable ingredients: an activator species, taking part of the positive feedback process that speeds up its own changes, an inhibitory process that exerts control on the positive feedback loop, and a larger diffusive range for the inhibition compared to the activation. In two species reaction-diffusion systems, Turing patterns may spontaneously grow if, for example, one of the chemicals is involved in its own creation (i.e., an autocatalytic reaction), and the other participates in a reaction that inhibits the previous activating process. Furthermore, it is necessary that the inhibitor diffuse much faster than the activator. The values of the reaction rates and the feeding (removal) of species specify the minimum amount by which the diffusion coefficient of the inhibitor must exceed that of the activator in order to observe these patterns [4].

Since the original paper by Turing, many two-species model reaction schemes fulfilling the kinetic conditions were proposed, and the corresponding reaction-diffusion systems were analyzed in the literature. The threshold value for the ratio of the diffusion coefficients is far from unity in most circumstances, and always strictly different than 1. However, in aqueous solutions all the chemicals involved in the reactions have nearly equal diffusion constants. This fact, as well as the great difficulties for sustaining constant nonequilibrium conditions in an spatially extended reactor [5], explain the long delay between the original proposition of Turing and the first clear observation of Turing patterns in laboratory experiments by Castets *et al.* [6]. Theoretical developments and numerical simulations based on model equations, but taking into account the real constraints of the experiments, were already available a few years before, and predicted the appearance of localized Turing structures [7,8]. Turing patterns were actually observed in experiments on the chlorite-iodide-malonic acid (CIMA) reaction, only after the inclusion of an exogenous mechanism that created the conditions on the diffusive ranges for their appearance. This was qualitatively pointed out in a paper by Lengyel and Epstein [9], using a simplified version of a previously developed model of the CIMA reaction which is completely based on empirical rate laws [10]. These papers set a theoretical framework to understand the appearance of Turing patterns in the experiments on the CIMA reaction [6,11]. The argument was that both the gel and the starch molecules used in the experiments to suppress nondiffusive transport and for visualization purposes, respectively, played an active role in the appearance of the patterns. Indeed it was the reversible complexation of iodide and iodine with large immobile molecular assemblies (starch molecules), that were responsible for the necessary tuning of the "effective diffusion" constants. Under a set of assumptions that are only approximately fulfilled in the particular case of the CIMA reaction, Lengyel and Epstein provided a more quantitative support to the idea of the effect of the complexing agent (CA) on the Hopf and Turing bifurcations [12]. More recently, systematic experiments performed in a gradient-free open reactor [13], demonstrated a close connection between the model predictions and the experimental results, in particular, with respect to the role of immobile complexing agents.

While the experimental observation of Turing patterns in controlled chemical reactors have triggered our theoretical understanding of these phenomena, opening up the possibil-

*Electronic address: strier@crpp-bordeaux.cnrs.fr; present address: Centre de Recherche Paul Pascal – CNRS (France).
†Electronic address: silvina@df.uba.ar

ity of technological applications, the question posed by Alan Turing [2] about its role in living organisms still remains open. Given that the autocatalytic chemical reactions substrate and product inhibition are commonly encountered in biochemical reactions, one of the bottle-necks in this realm is to find biologically plausible mechanisms for the tuning of the diffusion coefficients. It has been proposed that endogenous and exogenous molecular assemblies such as buffers [14,15], and the membrane-filled structure of the cell cytoplasm [16] may provide the ingredients for the rescaling of diffusion coefficients in *in vivo* systems, playing a similar role as the gel and the starch used in laboratory experiments [9,17]. Indeed, there is some evidence of spatial patterns in living organisms that are not scale invariant, as well as other indirect evidence that seems to justify its ultimate origin as the result of a diffusion driven instability of Turing type [4,18]. However, since the situation in biology is much more involved than the one in chemistry, the actual relevance of the Turing mechanism as a generator of patterns in biological systems is still uncertain.

Our aim in this paper is to formalize the above statements for a general reaction-diffusion system of activator-inhibitor or substrate-depleted types. Having in mind the experiments where Turing patterns were observed and the characteristics of the biological systems where Turing structures have been looked for, we suppose that some of the species involved are also taking part in a reversible reaction with a complexing agent. We also assume that the reaction with the CA occurs on a time scale that is small compared to that of the other process, which includes the rest of the chemical reactions, the feeding or removal of chemicals, and diffusion. As we have shown in Ref. [19], this hypothesis is verified in many situations of interest. We show in this paper how fast interactions deforms the set of parameter values for which a Turing instability occurs (the Turing space), by stabilizing stationary patterns in a region where the ratio of the free diffusion coefficients of the activator and the inhibitor can be set to 1, or even consider cases where the free diffusion of the activator is larger than that of the inhibitor. In contrast to the previous closely related work of Ref. [12], where the relevant two-variable system of reaction-diffusion equations were derived for a particularly simple limiting case to avoid mathematical difficulties, in this paper a more general set of equations are obtained using the multiple-time scale approach developed in Refs [17,19]. This makes it possible to remove some simplifying assumptions used in Ref. [12], that reduce the range of validity of their results. In fact, we can handle the case where the CA diffuses, or where the CA is not in excess, and so allow for large variations of the concentration of the CA in the course of the evolution. Also we consider the effect of reversible complexation of both the activator and the inhibitor. This should make our results to be more widely applicable not only with regard to laboratory experiments, where mobile dyes could be an option, and where large excess is not always a good approximation, but also in biological situations, where the overall behavior may be qualitatively different depending on the transport properties of the CA involved [20], or when the role of CA is played by enzymes which are often in small concentrations compared with the metabolites.

After deriving the rescaled equations (i.e., the reduced system obtained after the fast dynamics is properly collapsed onto the variables that evolve at a relatively slow pace [17,19]), we proceed further with the analysis providing a series of analytical relations, and a procedure to be followed in this sort of problems to assess if the appearance of stable patterns can be expected for a given system. For a particular example, we also show the agreement between the results of the reduced approach with that of the full model.

The paper is organized as follows. In Sec. II we present the analytical results on the stabilization of Turing patterns by the action of the CA. After a brief review of the conditions for the emergence of Turing patterns in a generic two species model (Sec. II A), we show how the set of rescaled reaction-diffusion equations that take into account the presence of rapid CA are obtained (Sec. II B). Then, we perform the linear stability analysis on the rescaled equations and the new conditions for the Turing instability are derived (Sec. II C). Finally, in Sec. III, we show an example of biological relevance in order to illustrate the main results. We discuss the central points in the conclusions.

II. THE MODEL

A. Introductory remarks

The general form of a two species reaction-diffusion system is

$$\begin{aligned} \frac{\partial u}{\partial t} &= f(u,v) + D_u \nabla^2 u, \\ \frac{\partial v}{\partial t} &= g(u,v) + D_v \nabla^2 v, \end{aligned} \tag{1}$$

where u and v stand for the concentration of molecules of species $\mathcal{U}$ and $\mathcal{V}$, respectively, and D_u and D_v for their diffusion coefficient. These equations reflect that the local concentration of a given species can change as a result of the chemical reactions, and to a thermal transport process (diffusion). The $f(u,v)$ and $g(u,v)$ functions are constructed from the proposed reaction scheme using the law of mass action or are determined empirically.

The study of Turing patterns starts from the assumption that a homogeneous fixed point solution (u_0,v_0) exists [i.e., the nullclines $f(u,v)=0$ and $g(u,v)=0$ intersect at (u_0,v_0)]. The signs of the coefficients of the spatially homogeneous dynamical system (1), linearized around the fixed point solution, give important information about the destabilization mechanism of the homogeneous solution (u_0,v_0). It can be shown that when the signs of the stability matrix, whose rows are the gradients of f and g with respect to u and v evaluated at the fixed point (e.g., $f_u \equiv \partial f/\partial u]_{(u_0,v_0)}$) are given by

$$A \equiv \begin{pmatrix} f_u & f_v \\ g_u & g_v \end{pmatrix} = \begin{pmatrix} + & + \\ - & - \end{pmatrix} or \begin{pmatrix} + & - \\ + & - \end{pmatrix}, \tag{2}$$

it is then possible to find a Turing-like instability whenever the rate constant and the diffusion coefficients satisfy certain constraints. The cases in Eq. (2) correspond to the substrate-

TABLE I. Conditions on the reaction kinetics at the fixed point and the diffusion process that guarantee the appearance of Turing patterns in generic two-species reaction-diffusion systems described by Eq. (1) (see Ref. [4]).

Stable homogeneous	Unstable inhomogeneous
$f_u+g_v<0$	$df_u+g_v>0$
$f_ug_v-f_vg_u>0$	$(df_u+g_v)^2\geq 4d(f_ug_v-f_vg_u)$

depleted and activator-inhibitor classes, respectively [21]. The conditions for the existence of Turing patterns state that the homogeneous fixed point solution (u_0,v_0) must be stable under small homogeneous perturbations, but become unstable to spatially inhomogeneous disturbances. In other words, the eigenvalues of the linear operator that is obtained by linearizing the full set of Eqs. (1) around the fixed point solution must be negative when the diffusion terms are absent (homogeneous situation), but when they are present, the stationary state has to become unstable to periodic perturbations of wave number $\mathbf{k}\neq 0$. So, a necessary and sufficient condition for the existence of Turing patterns is that the real part of the largest eigenvalue of this linear operator be positive for some $\mathbf{k}\neq 0$, but remain negative for $\mathbf{k}=0$. We summarize in Table I the conditions under which these requirements are fulfilled [4], where we have defined the dimensionless diffusion ratio $d=D_v/D_u$. Note that the conditions in the first row of this table necessarily imply that $d>1$. It follows from the second row that there is a critical ratio of diffusion coefficients (d_c), above which the conditions are fulfilled. In this way the fixed point solution will become linearly unstable under inhomogeneous perturbations of finite wave numbers within a certain range. Below the critical ratio, there is no combination of the parameters of the model that can give rise to Turing patterns.

B. Adding rapid complexing agents

When $d<d_c$ the Turing space, that is, the parameter domain where the otherwise stable stationary state is linearly unstable to a nonuniform perturbation, contains no points. As we have mentioned earlier, the problem is that while $d\sim 1$ in most circumstances, the value d_c is in general much greater than one. Thus, if we restrict ourselves to schemes similar to Eq. (1), then it would be unlikely to observe these patterns. In the same spirit of Refs. [9,12,14,22,23], we consider that each morphogen undergoes a reversible reaction with some CA. Taking CA into account is clearly justified in those cases where we know exactly their identity. This occurs, for example, in the CIMA reaction, but also in many biochemical pathways where opposite feedback loops of activation and inhibition coexist with interactions with known endogenous buffers and enzymes, as in the glycolytic pathway [24]. In these situations, the procedure that we will describe below, allows us to establish if the interaction with the CA makes the appearance of Turing patterns more or less likely. In other cases, where a detailed knowledge of the reaction scheme is not available, but where the existence of CA can be taken for granted [25], the addition of a set of reactions with CAs can be used to determine the range of dissociation constants and CA concentration where Turing instabilities could occur.

There are two cases worth studying. The case in which both, the activator and the inhibitor react (with different affinities) with the *same* CA [26], and the case in which each species reacts with a *different* CA [27]. While the first case introduces another source of coupling between $\mathcal{U}$ and $\mathcal{V}$ that leads to the presence of cross-diffusion terms in the rescaled equations, the second case is easier to analyze because the rescaling of the equations is decoupled. For simplicity, we will consider only the second case. The proposed interaction with the CA has the following simple form:

$$S+B_S \underset{k_S^-}{\overset{k_S^+}{\rightleftharpoons}} C_S, \tag{3}$$

where S can be either $\mathcal{U}$ or $\mathcal{V}$, B_S stands for the CA, and C_S for the complex formed between S and B_S. While in many real systems the mobility of the CA is small, and can be neglected in front of those of the $\mathcal{U}$ and $\mathcal{V}$ molecules, in other situations, the mobility is noticeable and cannot be underestimated, because the overall behavior of the system may be qualitatively different depending on the transport properties of the CA involved, as we mentioned before. So, we will consider the diffusive transport of the CA, and assume that the reaction with these CAs occurs much faster than any other process in the system, and that their mobility is not affected by the binding with S. With this in mind, defining $b_u=[B_{\mathcal{U}}]$, $c_u=[C_{\mathcal{U}}]$, $b_v=[B_{\mathcal{V}}]$ and $c_v=[C_{\mathcal{V}}]$, the reaction diffusion system becomes

$$\frac{\partial u}{\partial t}=f(u,v)+r^u(u,b_u)+D_u\nabla^2 u, \tag{4}$$

$$\frac{\partial v}{\partial t}=g(u,v)+r^v(v,b_v)+D_v\nabla^2 v, \tag{5}$$

$$\frac{\partial b_u}{\partial t}=r^u(s,b_u)+D_{b_u}\nabla^2 b_u, \tag{6}$$

$$\frac{\partial c_u}{\partial t}=-r^u(s,b_u)+D_{b_u}\nabla^2 c_u, \tag{7}$$

$$\frac{\partial b_v}{\partial t}=r^v(s,b_v)+D_{b_v}\nabla^2 b_v, \tag{8}$$

$$\frac{\partial c_v}{\partial t}=-r^v(s,b_v)+D_{b_v}\nabla^2 c_v. \tag{9}$$

Letting the total amount of the CA that reacts with $S=\mathcal{U},\mathcal{V}$ to be denoted by $b_s^T=b_s+c_s$ $(s=u,v)$, the fast reaction with the complexing agent is described by

$$\varepsilon r^s(s,b_s)=-k_s^+ s\,b_s+k_s^-(b_s^T-b_s),\quad s=u,v, \tag{10}$$

where $0<\varepsilon\ll 1$ makes explicit the fact that reactions with CAs are fast. Because of the absence of any source or sink

term for the CA in Eqs. (6) to (9), its total amount remains constant during the whole evolution. Furthermore, if we assume that initially, the distribution of b_s^T is uniform in space, these equations also imply the homogeneity of b_s^T throughout the evolution. Taking advantage of the different timescales present in the system (4)–(9), and following the procedure described in Ref. [17], we perform a regular perturbative expansion on the small parameter ε. In this way, we are focusing on the outer solution that is reached after a small transient where the fast variables (the concentrations of the complexing agents) rapidly approach a stable manifold, which is uniquely defined by algebraic equilibrium relations [28]. The reduced system of rescaled evolution equations for the slow time-scale dynamics obtained from Refs. [4–9] is given by

$$\begin{aligned}\frac{\partial u}{\partial t} &= \frac{f(u,v)}{1+A_u(u)} + d_u(u)\nabla^2 u - H_u(u)\vec{\nabla}u\cdot\vec{\nabla}u,\\ \frac{\partial v}{\partial t} &= \frac{g(u,v)}{1+A_v(v)} + d_v(v)\nabla^2 v - H_v(v)\vec{\nabla}v\cdot\vec{\nabla}v,\end{aligned} \tag{11}$$

where we have defined

$$\begin{aligned}d_s(s) &= \frac{D_s + A_s(s)D_{b_s}}{1+A_s(s)},\\ H_s(s) &= \frac{2D_{b_s}A_s(s)}{(k_s^d+s)[1+A_s(s)]},\\ A_s(s) &= \frac{k_s^d b_s^T}{(k_s^d+s)^2}\end{aligned} \tag{12}$$

and $k_s^d = k_s^-/k_s^+$ stands for the dissociation constant ($s=u,v$). Equations (11) were also derived in detail in the context of calcium waves (see Ref. [29], p. 342). The CA concentrations are —after a short transient— slaved to u and v via algebraic relations (see Ref. [19]). Notice that the system of equations (11) is no longer of reaction-diffusion type, except for some limiting cases as the one treated by Ref. [12], and others discussed in Ref. [19]. For simplicity, in the following we will consider only the case of one space dimension. We will look for a nonlinear transformation in order to get rid of the nonlinear term proportional to the squared gradient of s in Eq. (11). Following Sneyd *et al.* [22], we propose

$$u = \psi(U), \quad v = \theta(V), \tag{13}$$

where ψ and θ are unknown functions to be suitably determined. We will constrain the space of possible transformations to those that are —at least— twice differentiable and monotonically increasing. The degrees of freedom can be reduced by a reasonable requirement: in the absence of complexation, or when the CA can be considered as immobile, these functions should reduce to the identity transformation [see Eq. (14) below]. The first equation in Eq. (11) can now be written as

$$\psi'\frac{\partial U}{\partial t} = \frac{f(\psi,\theta)}{1+A_u(\psi)} + d_u(\psi)\psi'\frac{\partial^2 U}{\partial x^2} + \left[d_u(\psi)\psi'' - H_u(\psi)\psi'^{\,2}\right]\times\left(\frac{\partial U}{\partial x}\right)^2, \tag{14}$$

where x denotes the spatial coordinate, ψ' and ψ'' denote, respectively, the first and second derivatives of ψ with respect to U. The relations for v may be obtained from Eq. (14) by replacing $\psi\to\theta$ and $U\to V$. If the unknown function ψ satisfies the following differential equation [22]:

$$d_u(\psi)\psi'' = H_u(\psi)\psi'^{\,2}, \tag{15}$$

then, the term that comes from the squared gradient of u is automatically removed. The integration of equation (15) yields

$$\psi D_u - \frac{b_u^T k_u^d D_{b_u}}{k_u^d+\psi} = \alpha U + \alpha', \tag{16}$$

where the constants of integration α and α' can be determined using the constraints that we imposed on the proposed transformation, that is,

$$\alpha = D_u, \alpha' = 0. \tag{17}$$

Thus, we finally obtain the following equations for U and V:

$$\begin{aligned}\frac{\partial U}{\partial t} &= F(U,V) + d_u(\psi(U))\frac{\partial^2 U}{\partial x^2},\\ \frac{\partial V}{\partial t} &= G(U,V) + d_v(\theta(V))\frac{\partial^2 V}{\partial x^2},\end{aligned} \tag{18}$$

where

$$F(U,V) = \frac{1}{\psi'}\frac{f(\psi,\theta)}{1+A_u(\psi)} = d_u(\psi)f(\psi,\theta)/D_u, \tag{19}$$

$$G(U,V) = \frac{1}{\theta'}\frac{g(\psi,\theta)}{1+A_v(\theta)} = d_v(\theta)g(\psi,\theta)/D_v. \tag{20}$$

A couple of things are worthy of remark here. First, as can be appreciated from their definition [see Eq. (12)], the functions $d_s(s)$, that play the role of the diffusivities in the evolution equations of U and V represent a density dependent weighted average between the diffusion coefficients of the species S and that of the CA with which S reacts. If the diffusion coefficient of the CA is equal to that of S, then $d_s(s)=D_s$, which makes sense because in this situation its mobility is not affected by the binding to the CA. If, on the contrary, the CA is immobile, then the effective diffusion coefficient of S is simply its free diffusion coefficient divided by the same rescaling factor that appears in the reaction term. In this case the rescaling factor can also be derived from a microscopic analysis of the system [19], and may be associated to the average amount by which the time of free diffusive motion is reduced by the interaction with the CA.

The second point we want to stress is that the homogeneous fixed point solutions for u and v after rescaling coincide with the homogeneous stationary solutions of the reaction-diffusion system in the absence of CA, as can be seen, for example, from the last two definitions of the new reaction terms in the transformed equations. Finally, given that the transformation (13) is monotonous, it is clear that homogeneous fixed point solutions in the $u-v$ variables correspond to homogeneous fixed point solutions in the $U-V$ space, and the same holds for patterns. Thus, the presence or absence of a pattern in the $U-V$ space and in the original $u-v$ are in a one-to-one correspondence.

We write for completeness the explicit form of the transformation from the concentration $u(x,t)$ to the function $U(x,t)$ and viceversa (we avoid writing the twin condition for $v \leftrightarrow V$):

$$U = \psi^{-1}(u) = u - \frac{k_d b_u^T D_{b_u}}{d_u(k_d + u)},$$

$$u = \psi(U) = \frac{U - k_d}{2} + \frac{1}{2}\sqrt{(U + k_d)^2 + 4k_d b_u^T D_{b_u}/D_u}.$$

Given that $f[\psi(U_0), \theta(V_0)] = 0$ and $g[\psi(U_0), \theta(V_0)] = 0$, where $U_0 = \psi^{-1}(u_0)$ and $V_0 = \theta^{-1}(v_0)$, it follows that at the homogeneous steady state:

$$F_U = \frac{d_u(u_0)}{D_u} f_u \psi'(U_0), \qquad F_V = \frac{d_u(u_0)}{D_u} f_v \theta'(V_0),$$

$$G_U = \frac{d_v(v_0)}{D_v} g_u \psi'(U_0), \qquad G_V = \frac{d_v(v_0)}{D_v} g_v \theta'(V_0).$$

Then we conclude that the (transformed) kinetic functions that are obtained for the rescaled equations, preserve the same structure of signs in the stability matrix as the original one. This result follows from the fact that the proposed reactions with CA do not change the characteristics of the interaction between the morphogens. By varying the available free activator-inhibitor molecules, CAs may modify the probability of reactive collisions embodied in the weight of the reaction terms, but not the same kind of interaction as reflected in these derivatives.

C. Linear stability analysis with complexing agents included

The linear analysis near the homogeneous fixed point solution of Eq. (18) is analogous to the one performed with the system (1). To assess the effect of CAs, it is convenient to express the conditions for the Turing instability when mobile CAs are present, in terms of the conditions that we required for the original system without CAs. We summarize the results in Table II, where we have scaled out a positive prefactor from the condition on the determinant of the stability matrix, and defined the dimensionless ratios $R \equiv [d_u(u_0)/d_v(u_0)]\mathcal{D}$ and $\mathcal{D} \equiv d(\psi'/\theta')$. Comparing Tables I and II we may see that the effect of the reactions with the CAs appears only through the positive factor R. As we will see now, its presence introduces important changes regarding the structure of the Turing space.

TABLE II. Modified conditions for the appearance of Turing patterns when reactions with complexing agents are taken into account.

Stable homogeneous	Unstable inhomogeneous
$Rf_u + g_v < 0$	$\mathcal{D}f_u + g_v > 0$
$f_u g_v - f_v g_u > 0$	$(\mathcal{D}f_u + g_v)^2 \geqslant 4\mathcal{D}(f_u g_v - f_v g_u)$

In spite of the algebraic complexity of the terms in Table II and of the cumbersome transformations ψ and θ, at least numerically, it is now a straightforward exercise to compute the Turing space. Namely, one only needs to grid the space of parameters, and plug into the relations of Table II all the different parameter combinations and save those that verify all conditions simultaneously. Note that for the inequalities of the first row of Table II to hold simultaneously, it is necessary that $d_v(v_0) > d_u(u_0)$. This necessary condition represents the extension of the former $D_v > D_u$ condition to the case where reactions with CAs are taken into account. But now it is no longer necessary for the free diffusion of the inhibitor to be larger than that of the activator. There is a key difference between them: while the value of d is fixed, and thus, the condition $d > d_c$ is unlikely to be reached in the absence of CAs, the value of $\mathcal{D}$ can be driven above threshold because of its dependence on genuine tunable variables, such as the CA concentration. A last point worth to remark concerns the effect of CAs on the wave number that corresponds to the most unstable mode k_c. It readily follows that

$$k_c^2 = \sqrt{\psi'\theta'}\, k_{c,0}^2, \qquad k_{c,0}^2 = \sqrt{\frac{f_u g_v - f_v g_u}{D_u D_v}}, \tag{21}$$

where $k_{c,0}$ corresponds to the critical wave number in the absence of complexing agents. Thus, the departures of the wavelength of the patterns because of the presence of CAs are embodied through the first factor, which is equal to unity only when CAs do not diffuse. This agrees with the calculation of [30] for the CIMA reaction. If the dissociation constants are known, Eq. (21) may be used to estimate the diffusion coefficient of CAs, by varying their concentration, and comparing the changes exerted on the macroscopic length with those predicted by Eq. (21).

As a simple illustration of the above results, let us consider the reaction diffusion system (4)–(9) with immobile CAs, formally setting $D_{b_u} = D_{b_v} = 0$. Then, $\psi' = \theta' = 1$, and the four conditions for the Turing instability now reads

$$R f_u + g_v < 0, \tag{22}$$

$$f_u g_v - f_v g_u > 0, \tag{23}$$

$$d f_u + g_v > 0, \tag{24}$$

$$(d f_u + g_v)^2 \geqslant 4d(f_u g_v - f_v g_u), \tag{25}$$

where in this case R is simply given by

$$R = R(u_0, v_0) = \frac{1 + A_v(v_0)}{1 + A_u(u_0)}. \tag{26}$$

Except for Eq. (22), these restrictions look similar to the ones obtained in Ref. [4]. Note that the rescaling factor obtained by Ref. [12] is a limiting case of Eq. (26), when the dependence on the fixed point can be neglected i.e., the concentrations at the fixed point are negligible with respect to the dissociating constant), and no interaction of v with a CA exist. We can see from these relations what the starch molecules, or other immobile CAs do in order to allow the observation of patterns in experiments: they simply set a value of R sufficiently lower than 1, so as to permit the stabilization of patterns with $d \sim 1$. As we have mentioned, while the free diffusion ratio cannot be tuned, it is possible for the ratio R to be manipulated experimentally, taking advantage of its dependence on the total concentration of CAs. The role of immobile complexing agents can be interpreted more clearly. Note that, in such a case, the rescaling enters into the equations for u and v through a multiplicative factor on the right-hand side of Eq. (11). Then it is clear that the stationary solutions cannot change by the presence of the immobile CAs. Thus, given that the Turing bifurcation involves only stationary solutions, the point in the space of parameters where the Turing bifurcation occurs also remains the same. This can also be appreciated directly from the condition on the determinant of the stability matrix, because the point in the parameter space where the determinant is zero (i.e., where the Turing bifurcation occurs through a pitchfork or a transcritical bifurcation) is not changed by the presence of the prefactor due to the complexing agents. Instead, what the immobile CAs do is to change the place where the Hopf bifurcation with $k=0$ occurs (another instability that the fixed point can suffer), by modifying the sign of the trace of the matrix $\mathcal{A}$ [31]. In this way, a positive trace (an unstable homogeneous fixed point surrounded by a closed orbit) can become negative (a stable fixed point) because of the immobile CA. Then, when this stable homogeneous fixed point solution collides with or splits up into other stationary inhomogeneous solutions (as it occurs in transcritical and pitchfork bifurcations), the latter solutions will inherit the stability of the homogeneous fixed point solution. If the complexing agents are mobile, in principle, new stationary solutions could be created by the presence of the CA. A large number of possibilities arises in this case, whose analysis goes beyond the aims of the present work.

III. APPLICATION: THE SCHNACKENBERG MODEL (SM)

In order to proceed further with the analysis of the last example we need to restrict ourselves to a particular reaction-diffusion model. We analyze in this section, an extensively studied model in connection with Turing patterns [4], to which we add a set of reactions with buffers. This extended model reads

$$\mathcal{X} \underset{k-1}{\overset{k+1}{\rightleftharpoons}} A, \quad B \overset{k_2}{\rightarrow} \mathcal{Y}, \quad 2\mathcal{X} + \mathcal{Y} \overset{k_3}{\rightarrow} 3\mathcal{X}, \tag{27}$$

$$\mathcal{X} + \mathcal{B}_X \underset{k_{-4}^X/\varepsilon}{\overset{k_{+4}^X/\varepsilon}{\rightleftharpoons}} \mathcal{C}_X, \tag{28}$$

$$\mathcal{Y} + \mathcal{B}_Y \underset{k_{-4}^Y/\varepsilon}{\overset{k_{+4}^Y/\varepsilon}{\rightleftharpoons}} \mathcal{C}_Y. \tag{29}$$

The reaction scheme (27) constitutes the so-called Schnackenberg model (SM). If the concentration of A and B are kept at certain nonequilibrium values, the SM displays oscillations in the concentration of $\mathcal{X}$ and $\mathcal{Y}$. We add to the model the set of fast reactions with buffers (28) and (29). This extended model has many advantages. On one hand, it is simple enough to allow us to obtain the boundary of the Turing space analytically, making it possible to see how its position changes as a function of the concentration of the buffers. On the other hand, it is intrinsically interesting as a plausible model behind the Turing-like patterns found in some living organisms. Indeed, an important motivation for studying this system is the idea that a similar mechanism controls some features of the unicellular algae Acetabularia [4,32]. While this simple model reproduces some of the experimental observations, such as the intrinsic wavelength of the pattern or the window of external calcium concentration where the patterns can be formed, one of its weak points, is the unrealistic requirement on the ratio between the free diffusion coefficients of the ions (probably Ca^{++} and H^+) that would play the role of morphogens. However, it is reasonable to suppose that these ions (or even cAMP, which is another plausible morphogen instead of H^+) are buffered in the course of the reactions, and that the system with rescaled diffusion and reactions permits the formation of patterns with a reasonable ratio between the free diffusion coefficients. We can take the values of real intracellular buffers, such as troponin-C or calmodulin (see Ref. [29], and references therein), to have an idea of the typical order of magnitude of such rescaling. Reasonable ranges for the concentration of these two buffers are within 10 and 100 μM, with dissociation constants between 1 and 5 μM [33]. Also, both buffers diffuse in the cytoplasm at rates that are lower than 20 $\mu m^2/s$, a value which is at least one order of magnitude below that of any of the proposed morphogens. The rest of the kinetic and feeding parameters are considered to vary in the same ranges as in Ref. [4].

In the remainder of this section we first sketch how the reduction procedure is performed considering, for simplicity $[\mathcal{B}_Y]=0$, and comparing the main results with those of the full system (Sec. III A). We then use the results of Sec. II to find and analyze the Turing space of the reduced set of equations (Sec. III B).

A. The reduced equations

Using mass action kinetics and writing $X=[\mathcal{X}]$, $Y=[\mathcal{Y}]$, $A=[A]$, $B=[B]$, $B_X=[\mathcal{B}_X]$, and $C_X=[\mathcal{C}_X]$, the reaction-diffusion equations associated to the scheme (27)–(29) are

$$\frac{\partial X}{\partial \tau} = k_{-1}A - k_1 X + k_3 X^2 Y - \frac{1}{\varepsilon}(k_4 X B_X - k_{-4} C_X) + D_X \nabla^2 X, \tag{30}$$

$$\frac{\partial Y}{\partial \tau} = k_2 B - k_3 X^2 Y + D_Y \nabla^2 Y, \tag{31}$$

$$\frac{\partial B_X}{\partial \tau} = -\frac{1}{\varepsilon}(k_4 X B_X - k_{-4} C_X), \tag{32}$$

$$\frac{\partial C_X}{\partial \tau} = \frac{1}{\varepsilon}(k_4 X B_X - k_{-4} C_X). \tag{33}$$

In order to simplify the analysis of the system we introduce dimensionless variables

$$u = X\kappa,\ v = Y\kappa,\ t = \frac{D_X}{L^2}\tau,\ d = D_Y/D_X,$$
$$a = \frac{k_{-1}A}{k_1}\kappa,\ b = \frac{k_{-1}B}{k_1}\kappa,\ \kappa = \left(\frac{k_3}{k_1}\right)^{1/2},\ \gamma = k_1\frac{L^2}{D_X},$$
$$b_u = \frac{B_X}{B_T},\ \alpha = k_{-4}\frac{L^2}{D_X},\ \eta = \alpha\kappa B_T,\ \beta = \frac{k_4}{\kappa k_{-4}},$$

where B_T is the total buffer concentration and L is some characteristic length. In terms of these dimensionless quantities, (30)–(33) can be rewritten as

$$\frac{\partial u}{\partial t} = \gamma(a - u + u^2 v) + \frac{\eta}{\varepsilon}(1 - b_u - \beta u b_u) + \nabla^2 u, \tag{34}$$

$$\frac{\partial v}{\partial t} = \gamma(b - u^2 v) + d\nabla^2 v, \tag{35}$$

$$\frac{\partial b_u}{\partial t} = \frac{\alpha}{\varepsilon}(1 - b_u - \beta u b_u), \tag{36}$$

where we have used the conservation of the amount of buffer in its two forms. We propose an expansion of the buffer concentration in powers of the small parameter ε: $b_u = b_u^{(0)} + \varepsilon b_u^{(1)} + \cdots$. Then, it follows that $b_u^{(0)} = (1+\beta u)^{-1}$, and $b_u^{(1)} = (\beta/\alpha b_u^{(0)})(\partial u/\partial t)$. After a short transient, the evolution occurs on a slow manifold and is properly described by

$$\frac{\partial u}{\partial t} = \gamma r(u)(a - u + u^2 v) + r(u)\nabla^2 u, \tag{37}$$

$$\frac{\partial v}{\partial t} = \gamma(b - u^2 v) + d\nabla^2 v, \tag{38}$$

where

$$r(u) = \frac{1}{1 + \mu(1+\beta u)^{-2}},\ \mu = \frac{\eta\beta}{\alpha} = \frac{B_T}{k_u^d}. \tag{39}$$

The only parameters that can be regarded as truly tunable are a, b, and μ, because the first two are proportional to the concentrations of the infinite sources to which the system is supposed to be connected, and the latter, to the total concentration of buffer. Equations (37) and (38) make clear that even for $d \approx 1$, the effective diffusion rates of u and v may differ, in particular, if $r(u)$ is sufficiently low. We may also see that the reaction terms are also rescaled by the reduction procedure. The (homogeneous) fixed point solution of system (34)–(36) [and also of Eqs. (37) and (38)] can be written in terms of a and b as $u_0 = a+b$, $v_0 = b/(a+b)^2$, and $b_{u_0} = [1 + \beta(a+b)]^{-1}$. Applying the linear stability conditions sumarized in Table II, it is now possible to obtain vectors of parameters that belong to the Turing space. We show in Fig. 1 the results of a numerical integration of Eqs. (37) and (38) for $d=1$ and a set of parameter values ($a=0.02$, $b=0.3$, $\gamma = 500$, $\mu = 10$, $\beta = 0.1$) inside the Turing space obtained as described. We can observe the evolution from a random initial condition near the homogeneous fixed point towards a Turing pattern.

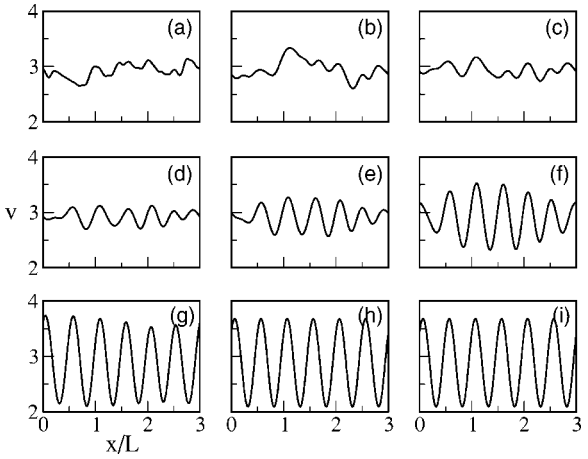

FIG. 1. Time evolution of the dimensionless concentration profile v towards a Turing pattern in the Schnackenberg model with CAs. The space variable x/L is also adimensional (see the lower left graph). Frames (a) – (i) correspond, respectively, to times $t=0.008$, $t=0.04$, $t=0.08$, $t=0.24$, $t=0.4$, $t=0.6$, $t=1$, $t=4$, and $t=20$. The diffusion coefficient of the activator and the inhibitor were considered to be exactly equal ($d=1$). The initial condition is randomly distributed around the fixed point. Other parameters in the main text.

We study now whether the property mentioned earlier according to which the wavelength of the Turing pattern is independent of the CA concentration when the CA is immobile, also holds for the complete system of equations (30)–(33). To this end, we show in Fig. 2 the real part of the largest eigenvalue of the linear operator of Eqs. (34)–(36), for $\varepsilon = 0.0001$, $\alpha = 0.2$, and η between 20 and 40 (or equivalently, μ between 10 and 20). The rest of the parameters are as in Fig. 1. As can be seen, the predictions of the reduced model are verified by the full one, in particular, the invariance of the wavelength with the buffer concentration. As can be apreciated from this figure, the maximum value of k_c^2 is close to 160, which implies a wavelength of approximately 0.5. Again this value is close to the one that spontaneously emerges in the simulation of the reduced model, giving confidence on the reduction procedure. Interestingly, it is also

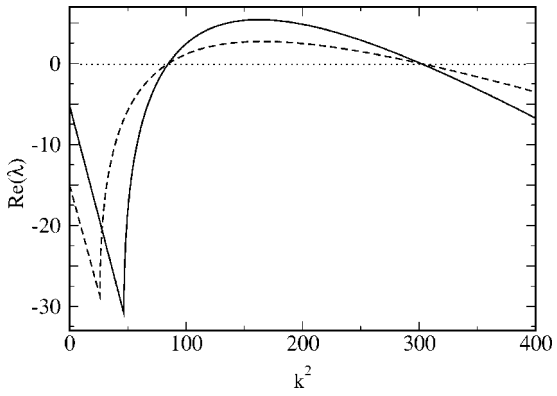

FIG. 2. Dispersion curves obtained from the complete system of equations (30)–(33): growth rate of a perturbation with (dimensionless) wave vector k for $\eta=20$ (solid curve) and $\eta=40$ (dashed curve). Both the band of unstable modes and the wavelength of the most unstable one ($2\pi/k_c$), are independent of the buffer concentration. This result persists even when $\eta\to 1/\epsilon$. When η is below ~ 15.65, the homogeneous fixed point loses stability, and the Turing bifurcation dissapears.

observed that the whole band of unstable modes results independent of the concentration of CA, and that for $k=0$ the system evolves towards the equilibrium solution. There is a critical concentration of complexing agent (a minimum of $\eta\sim 15.65$) that is needed to supress oscillations.

B. Analysis of the Turing space

Having shown that the reduced model is in fact a good representation of the whole system when ϵ is small, we now study the reduced equations (37) and (38) within the framework developed in Secs. II B and II C. The kinetic functions of the unbuffered system in this case are given by $f(u,v)=\gamma(a-u+u^2v)$ and $g(u,v)=\gamma(b-u^2v)$. Inserting them in Eqs. (22)–(25), together with the specific form of the parameter R that comes from the interaction of the morphogens with their respective CAs, we obtain the relations that determine the Turing space. Except for some limiting cases where the boundaries of the Turing space can be found analytically, in most cases we have to resort to numerical techniques. In the following, however, we will analyze one of these situations where analytical calculations are possible. To this end, we suppose that the concentrations of u and v are much smaller than k_u^d and k_v^d, respectively. In this circumstance, the dependence of R on the homogeneous fixed point can be neglected, and we are allowed to write $R\simeq(1+b_v^T/k_v^d)(1+b_u^T/k_u^d)^{-1}$. The set of points (a,b,R) that satisfy conditions (22)–(25) simultaneously (i.e., Turing space) can be shown to lie, for a fixed value of R, between two boundary curves in the (a,b) plane that are parametrically given defined by

$$\begin{aligned}[a_1(t),b_1(t)] &= \frac{t}{2R}(R-t^2,R+t^2),\\ [a_2(t),b_2(t)] &= \frac{t}{2}\left(1-\frac{2t}{\sqrt{d}}-\frac{t^2}{d},1+\frac{2t}{\sqrt{d}}+\frac{t^2}{d}\right).\end{aligned} \tag{40}$$

We show in Fig. 3 how the Turing space changes as a function of R for $d=2$. Depending on the value of R the Turing space can be enlarged or shrinked. Given that the value of d is fixed, we must find a critical value of R, R_c, below which the Turing space is nonempty. The explicit value of the R_c may be obtained as done in Ref. [4] (see p. 401), that is, by looking for a value of R such that $[a_i(t),b_i(t)]=(0,1)$ for both $i=1,2$ simultaneously at a fixed d value. It is straightforward to see then that $R_c=d(3+2\sqrt{2})^{-1}$.

IV. CONCLUSIONS

The general concept behind Turing-like instabilities is that of short-range activation with long-range inhibition [4]. In two-species activator-inhibitor reaction-diffusion systems, this requires that the inhibitor diffuse faster than the activator, at least by a critical amount that depends on the param-

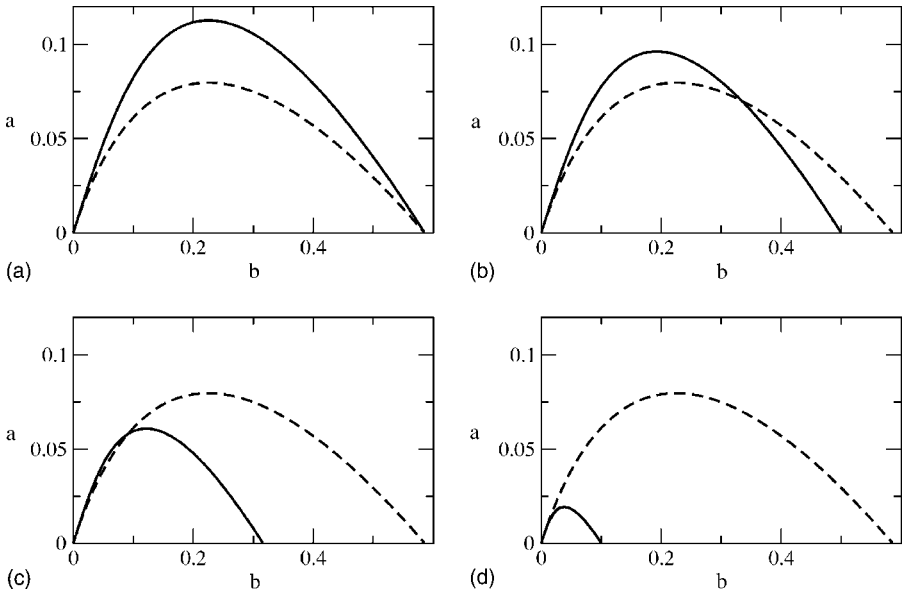

FIG. 3. The Turing space is the enclosed domain above the filled line [Eq. (41)] and below the dashed one [Eq. (40)]. In (a) $R=R_c$ and the Turing space contains no points. In (b); (c), and (d), $R=0.25, 0.1, 0.01,$ respectively. Note that the dashed line is the same for all the plots, because d has a fixed value (see the text).

eters of the reaction and feeding (source) terms. Several models have been proposed in the literature in order to explain real biological pattern formation processes by means of a Turing-like instability [4,18,32,34]. Some of these models lack a biological motivation, and others tend to capture quite schematically generic regulatory controls. In all these previous studies there is almost unrestricted freedom to choose kinetic parameters. Thus, even if the modeled patterns are astonishingly similar to the real ones, the similarity could be far from having any biological significance. On the other hand, even in those cases where there is some clue to the identities of the morphogens, the diffusion ratio is arbitrary tuned to "suitable" values, i.e., those lying beyond the instability threshold. Treating d as a bifurcation parameter necessarily implies that other reactions not explicitly considered, change the diffusion coefficients of the relevant molecules. The importance of these "ghost reactions" was first clearly stated by Lengyel and Epstein [9,12] to explain the experiments on the chlorite-iodide-malonic-acid (CIMA) reaction where Turing patterns were first convincingly observed in gel reactors [6,11]. A careful analysis of those experiments qualitatively showed that the diffusion coefficient of iodide was reduced by the interaction with the starch molecules loaded in the gel for visualization purposes. This would —they argued— provide the necessary difference between the diffusive rates of the morphogens involved, even though their free diffusion coefficients were similar.

Tuning the ratio of free diffusion coefficients to suitable values invoking the presence of a rescaling mechanism became customary in the literature on Turing patterns after the work of Ref. [9]. Following this approach, Turing patterns were predicted theoretically or observed numerically [16,18]. Our aim in this paper was to analyze the occurrence of Turing patterns including a detailed description of the reactions that can provide the necessary rescaling mechanism. There have been other works that also include these other reactions [9,10,12,30]. Although the analysis presented in Ref. [12] is similar to ours, it contains a set of assumptions that are excessively restrictive. In particular, assuming that the complexing agent is in large excess with respect to the activator species is not an essential feature for the appearance of patterns, neither is the fact that the complexing agent be tightly fixed to a large molecular network, and so, do not diffuse.

From a theoretical point of view, our paper removes the constraints of Ref. [12]. Namely, our goal is to provide explicit analytical formulas that can be used to "manipulate" the shape of the Turing space, in order to drive a given system towards a region where Turing patterns can develop. The degree of freedom that we use for this purpose (the fast reaction with the CA), is supported not only on the experimental evidence that comes from the CIMA reaction, but also on biological experiments where it has been demonstrated that endogenous or exogenous CAs tailor the repertoire of spatiotemporal organization that a system can display [35,36]. In particular, we have argued that the Schnackenberg model gives a qualitative framework for the problem of pattern formation in the unicellular algae Acetabularia. This problem had been studied in Ref. [4], but again, assuming an unrealistic ratio for the diffusion coefficients of the proposed morphogens. With our treatment, on the other hand, we start from a more general set of equations from which the effective ratio of diffusion coefficients is obtained, as well as the rescaling of the reaction terms. In this example we assumed that it was the interaction of the activatory species, with some endogeneous buffer (using characteristic values for the dissociation rates and concentration than those actually found in real cells), to be the process that made possible the appearance of a Turing structure. It is important to remark, however, that the application of the Schnackenberg model to the pattern formation process in the algae is not based on the knowledge of the real kinetic mechanisms involved, but on analytical convenience and predictive power [4]. Thus, our application of the method should be regarded as an illustrative example and not as proof of the relevance of Turing's ideas to the biological realm. In this regard, the situation is more favorable in Ref. [24], where it has been shown that Turing structures can indeed appear in cells because of the feedback loops involved in the glycolytic pathway. For the case of glycolysis, the kinetic mechanisms are quite well understood, and so the finding of patterns using mathematical models that accurately reproduce the temporal behavior, give genuine theoretical support to the existence of Turing structures at the cellular or supracellular level.

From an experimental point of view, the mathematical relations summarized in Table II can be used as a tool to choose between different sorts of CAs (with different dissociation constants and mobilities), or to regulate CA concentrations in order to see a stationary pattern. Even if the starting set of equations have serious limitations to capture the actual constraints of the experimental setup (for example, they implicitly assumed the validity of the pool chemical approximation [3]), we expect that this work can be used as a guide for finding Turing patterns in the laboratory, and for the design of experiments with new classes of chemical reactions.

It is believed that spatial patterns in biological systems are connected with the morphogenetic process. According to this view, the process of development is initiated by the formation of a Turing-like structure that plays the role of a prepattern for the subsequent process of development and growth. If Turing patterns are really relevant to a cell or a group of cells (as it is supposed to occur during the early stages of the development of the embryo), the mathematical relations derived here may illustrate the mechanism for the cell to switch the pattern on or off. Small changes in the production or degradation rates of certain proteins may lead to a sudden emergence or dissapearance of a global organization.

ACKNOWLEDGMENTS

We acknowledge useful conversations with P. De Kepper, J. Boissonade, G.B. Mindlin, and J.E. Pearson. This work has been funded by Universidad de Buenos Aires, ANPCyT-Argentina (Grant No. PICT03-08133) and National Institutes of Health (Grant No. GM65830). S.P.D is member of Carrera del Investigador Científico (CONICET). D.E.S acknowledges the financial support of the Ministry of Education of France and to the CRPP-CNRS where the final part of this work was done.

[1] P. Glansdorff, and I. Prigogine, *Thermodynamic Theory of Structure, Stability and Fluctuations* (Wiley, New York, 1971); G. Nicolis and I. Prigogine, *Self-Organization in NonEquilibrium Systems* (Wiley, New York, 1977).
[2] A. M. Turing, Philos. Trans. R. Soc. London, Ser. B **237**, 37 (1952).
[3] P. Borckmans, G. Dewel, A. De Wit, E. Dulos, J. Boissonade, F. Gauffre, and P. De Kepper, Int. J. Bifurcation Chaos Appl. Sci. Eng. **12** (11), 2307 (2002).
[4] J. D. Murray, *Mathematical Biology* (Springer, New York, 1989), Chap. 12.
[5] Z. Noszticzius, W. Horsthemke, B. McCormick, H. Swinney, and W. Tam, Nature (London) **329**, 619 (1987).
[6] V. Castets, E. Dulos, J. Boissonade, and P. De Kepper, Phys. Rev. Lett. **64**, 2953 (1990); P. De Kepper, V. Castets, E. Dulos, and J. Boissonade, Physica D **49**, 161 (1991).
[7] J. Boissonade, J. Phys. (Paris) **49**, 541 (1988).
[8] G. Dewel, D. Walgraef, and P. Borckmans, J. Chim. Phys. Phys.-Chim. Biol. **84**, 1335 (1987).
[9] I. Lengyel and I. Epstein, Science **251**, 650 (1991).
[10] A I. Lengyel, Gy. Rabai, and I. Epstein, J. Am. Chem. Soc. **112**, 4606 (1990); *ibid.* **112**, 9104 (1990).
[11] Q. Ouyang and H. Swinney, Nature (London) **352**, 610 (1991); Q. Ouyang and H. Swinney, Chaos **1**, 411 (1991).
[12] I. Lengyel and I. Epstein, Proc. Natl. Acad. Sci. U.S.A. **89**, 3977 (1992).
[13] B. Rudovics, E. Barillot, P. W. Davies, E. Dulos, J. Boissonade, and P. De Kepper, J. Phys. Chem. A **103**, 1790 (1999).
[14] J. Wagner and J. Keizer, Biophys. J. **67**, 447 (1994).
[15] N. L. Allbritton, T. Meyer, and L. Stryer, Science **258**, 1812 (1992).
[16] B. Hasslacher, R. Kapral, and A. Lawniczak, Chaos **3**, 7 (1993).
[17] D. E. Strier and S. P. Dawson, J. Chem. Phys. **112**, 2 (2000); *ibid.* **112**, 825 (2000).
[18] S. Kondo and R. Asai, Nature (London) **376**, 765 (1995).
[19] D. E. Strier, A. Chernomoretz, and S. P. Dawson, Phys. Rev. E **65**, 046233 (2002).
[20] For example, in experiments where different types of exogenous calcium buffers are added into the cytoplasm of cells, there could be a dramatic difference in the spatiotemporal organization according to the buffer's mobility. This fact has been clearly demonstrated in experiments done in oocytes, in which a transition from global calcium wave propagation to localized calcium release events (named puffs) could be induced by the addition of one type of mobile buffer (EGTA) but not of another one (BAPTA) [35].
[21] We will refer to the activator-inhibitor type in the rest of the paper, but exactly the same results hold for the other case.
[22] J. Sneyd, P. Dale, and A. Duffy, SIAM (Soc. Ind. Appl. Math.) J. Appl. Math. **58**, 4 (1998).
[23] G. Smith, Ph.D. thesis, University of California, Davis, 1996.
[24] D. E. Strier and S. P. Dawson (unpublished).
[25] This occurs, for example, in the case of cytosolic calcium dynamics, where, although the details of the interactions of calcium with specific membrane receptors are not fully known, yet it is known that buffers dramatically reduce the concentration of free calcium in the cytosol [29] and affect its diffusivity [15].
[26] This situation arises in biochemistry, where the same enzyme might bind, in different reaction steps, both, the inhibitor and the activator of a metabolic pathway [29].
[27] For example, the CIMA reaction is a particular case, where the starch molecules interact only with iodide [9]. This case is also relevant in biochemistry, with the CA representing two different buffers or enzymes.
[28] In Sec. III we analyze a particular example of this procedure. See Ref. [17] for a general treatment.
[29] J. Keener and J. Sneyd, *Mathematical Physiology* (Springer-Verlag, New York, 1998).
[30] W. Bruno and J.E. Pearson, Chaos **2**, 513 (1992).
[31] This was first recognized in Ref. [12].
[32] B. C. Goodwin, J. D. Murray, and D. Baldwin (unpublished).
[33] A. Michailova, F. DelPrincipe, M. Egger, and E. Niggli, Biophys. J. **83**, 3134 (2002).
[34] H. Meinhardt, in *On Growth and Form: Spatio-temporal Pattern Formation in Biology*, edited by M. A. J. Chaplain, G. D. Singh, and J. C. McLachlan (Wiley, London, 1999), pp. 129–148.
[35] N. Callamaras and I. Parker, EMBO J. **19**, 3608 (2000); J.S. Marchant and I. Parker, *ibid.* **20**, 65 (2001).
[36] J. Schnackenberg, J. Theor. Biol. **81** , 389 (1979).